JOURNAL OF CATALYSIS 124, 511–519 (1990)

Low-Temperature (144 K) ^{129}Xe NMR Studies of Catalytic Cracking Catalysts

T. T. P. CHEUNG

Phillips Research Center, Phillips Petroleum Company, Bartlesville, Oklahoma 74004

Received February 22, 1990; revised March 13, 1990

Xenon nuclear magnetic resonance (NMR) can be used to study the zeolitic component of fluidized catalytic cracking (FCC) catalysts. Interpretive methods from previous work on pure zeolite systems allow us to measure both the amount of zeolite present in the catalyst and the average volume of the zeolitic cages. A comparison of fresh and equilibrium catalysts shows that losses in zeolite content during cracking are primarily due to a decrease in the number of cages. The decrease in average cage volume is small in comparison. Catalysts prepared by an *in situ* zeolite growth process are more difficult to study using this method, but their zeolite content can still be measured.

I. INTRODUCTION

The high sensitivity of ^{129}Xe nuclear magnetic resonance (NMR) to the local electronic environment of adsorbed xenon atoms has provided a powerful means for characterization of zeolite materials (*1–7*). At 144 K, a temperature 17 K lower than the normal freezing point of xenon, we have shown (*7*) that information about the supercage size and the nature of the interactions between xenon and the cage wall in Y zeolites can be obtained. Also we have demonstrated (*8*) that ^{129}Xe NMR can be used to determine changes in the number and size of the supercages in steam-modified HY zeolites as a function of the extent of dealumination. In this report, we further extend the applications of low-temperature ^{129}Xe NMR to cracking catalysts.

Most of the commercial cracking catalysts are composed of Y zeolite embedded in amorphous matrices. Some catalysts are manufactured by dilution of pure zeolite (typically with micron-sized particles) with amorphous silica-alumina and inorganic binders. Others are prepared by growing the zeolite cages *in situ* by hydrothermal treatment of clays. In both cases, the zeolite material constitutes only a small percentage of the catalyst. While the zeolite material dominates the total micropore volume, a significant fraction of the internal pore volume is due to mesopores (~20–500 Å) and macropores (>500Å). Under the conditions of catalytic cracking and regeneration, there is a continuous degradation of the zeolite material in a catalyst. Vanadium in the feedstocks also causes the collapse of the zeolite framework. Coke formation may partially plug some of the zeolite pores. Therefore, one expects a reduction in the amount of zeolite material and the size of the zeolite cages in the catalyst.

There is an analogy between cracking catalysts and dealuminated HY zeolites in the sense that they both contain modified zeolite cages and mesopores. Our understanding of the ^{129}Xe NMR in steam-dealuminated zeolites (*8*) has facilitated interpretation of the results of the cracking catalysts. In this report, we examine three commercial catalysts, to which we refer as catalysts *A*, *B*, and *C*. We shall

0021-9517/90 $3.00

compare the xenon NMR of fresh and equilibrium catalysts. Our focus will be on the characterization of the zeolite content of these catalysts.

II. EXPERIMENTAL

Details of the experiments have been described elsewhere (*7–9*). Briefly, each sample was outgassed at 773 K for at least 10 h in a vacuum of 1×10^{-6} Torr before the introduction of xenon. The temperature of the sample in the NMR coil was lowered to 144 K in steps with sufficient time in between to allow the system to equilibrate. The amount of xenon adsorbed by the sample at 144 K, to which we shall refer as the xenon loading, was determined by subtraction of the amount of gaseous xenon remaining above the sample at that temperature from the total amount of xenon introduced to the sample. The xenon loading is given in terms of mmoles of xenon per gram of sample. The amount of gaseous xenon above the sample was calculated from the xenon adsorption isotherm measured at 143.3 K using a stirred liquid bath containing a solid–liquid mixture of *n*-pentane at its melting point.

NMR measurements of samples of different sizes of the same catalyst were used to check whether the cooling procedure was sufficient to produce equilibrium conditions for the samples. A larger sample is expected to take a longer time to reach equilibrium and nonequilibrium conditions can lead to rather different chemical shifts and linewidths for the same xenon loading. Our results (see Figs. 1–4), which are compiled from samples of different sizes, suggest that nonequilibrium problems are minimum. A more detailed discussion on this matter is given in Ref. (*9*).

^{129}Xe NMR chemical shifts are referenced to that of xenon gas extrapolated to zero pressure and room temperature by using the equation provided by Jameson *et al.* (*10*). The convention of a downfield resonance from the reference having a positive chemical shift is used.

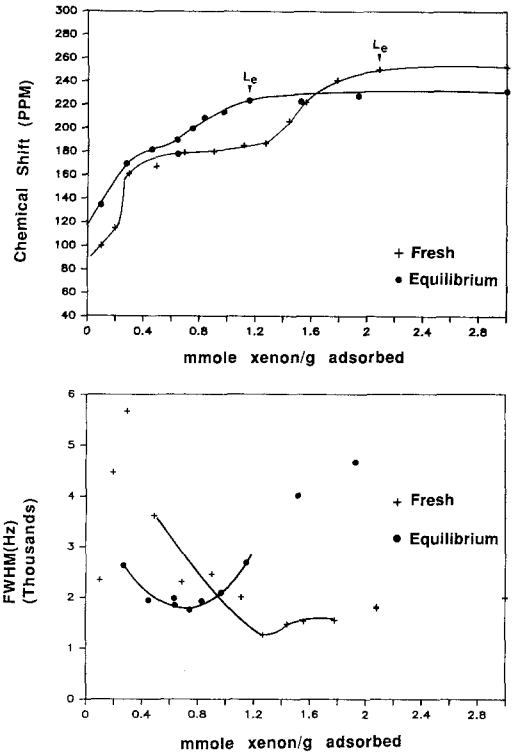

FIG. 1. ^{129}Xe NMR chemical shift and linewidth (FWHM) of xenon adsorbed in fresh and equilibrium catalyst *A* at 144 K as a function of xenon loading.

III. RESULTS AND DISCUSSION

Xenon Titration Curve in Cracking Catalysts

The ^{129}Xe NMR chemical shifts, σ, and the linewidths (full width at half maximum, FWHM) as a function of the xenon loading are given in Figs. 1 to 3, respectively, for catalysts *A*, *B*, and *C*. In each figure, we compare the results of the fresh catalyst with those of the equilibrium one. For comparison, the σ curve and the linewidths of xenon adsorbed in HY zeolite and steam-modified HY zeolite (*8*) are shown in Fig. 4.

A typical σ curve of a Y zeolite with (+1) cations may be divided into four regions (see Fig. 4). In region 1, at low loadings of xenon (less than 1 mmol Xe/gm for HY zeolite), the chemical shift increases more or less linearly with the xenon loading, corresponding to gaseous xenon inside the supercages.

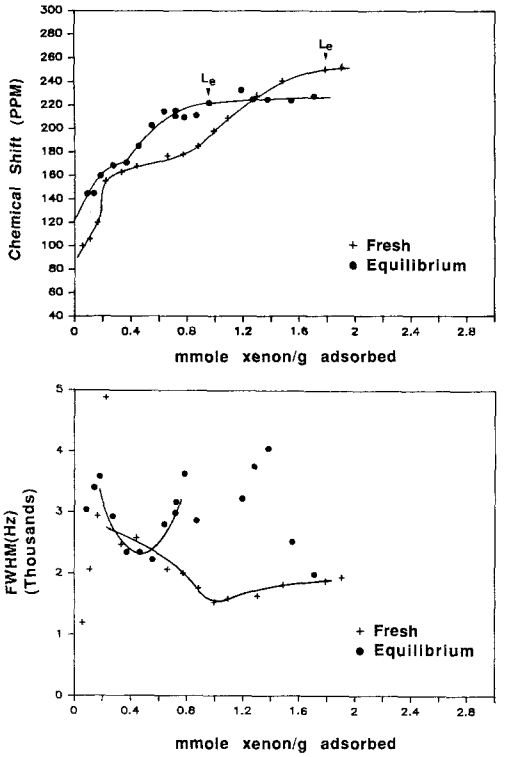

FIG. 2. ^{129}Xe NMR chemical shift and linewidth (FWHM) of xenon adsorbed in fresh and equilibrium catalyst *B* at 144 K as a function of xenon loading.

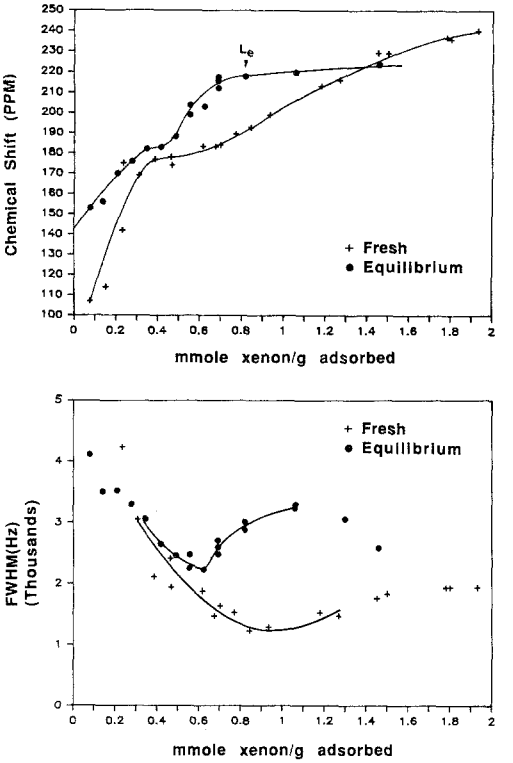

FIG. 3. ^{129}Xe NMR chemical shift and linewidth (FWHM) of xenon adsorbed in fresh and equilibrium catalyst *C* at 144 K as a function of xenon loading.

It is accompanied by a rapid increase in the linewidth. In region 2 (between 2 and 4.5 mmol Xe/gm for HY zeolite), the linewidth begins to decrease with little change in chemical shift. In region 3 (at loadings between 4.5 and 6.5 mmol Xe/gm for HY zeolite), the chemical shift increases sharply and a minimum in the linewidth appears. This is a consequence of the gas–liquid phase transition in the adsorbed xenon (*7*). The xenon loading at the minimum of the linewidth, L_m, marks the beginning of the rapid increase in the xenon partial pressure above the zeolite. The chemical shift at the linewidth minimum is found to be about 201 ppm downfield in HY, NaY, and steam-dealuminated HY zeolites, which suggests the existence of adsorbed xenon in a common physical state (*8*). Region 4 (above 6.5 mmol Xe/gm for HY zeolite) represents the complete filling of the supercages by xenon. The chemical shift and linewidth of the xenon inside the zeolite cages remains constant with further increase in loading, and excess xenon condenses as solid xenon outside the zeolite cages. The beginning of region 4 marks the ^{129}Xe NMR end-point, L_e, of the xenon titration of the supercages.

The σ curve of the steam-modified HY zeolite can be understood by considering the two ideal situations shown in Figs. 5a and 5b. In Fig. 5a, we compare the σ curve of a Y zeolite with (+1) cations with that of a physical mixture of the same zeolite with another material which does not absorb xenon. The steeper slope of the latter curve in region 1 is due to a higher xenon density in the zeolite cages at a given xenon loading. In Fig. 5b, we sketch the hypothetical σ curve of the same zeolite with smaller super-

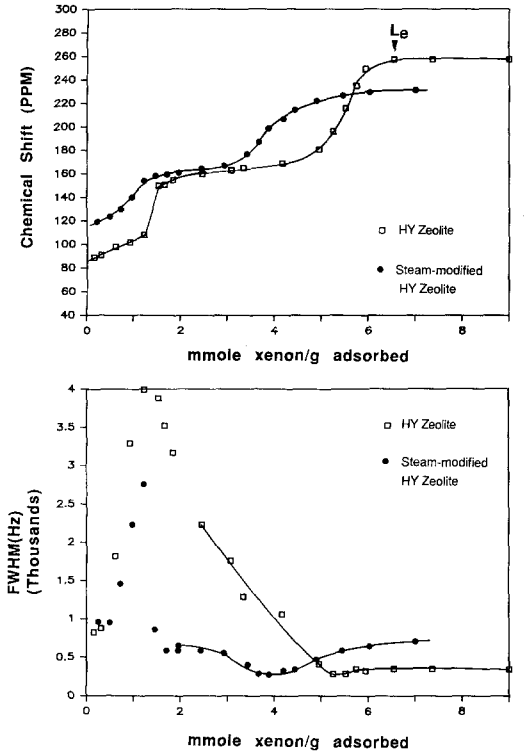

FIG. 4. ^{129}Xe NMR chemical shift and linewidth (FWHM) of xenon adsorbed in HY and steam-modified HY zeolite at 144 K as a function of xenon loading.

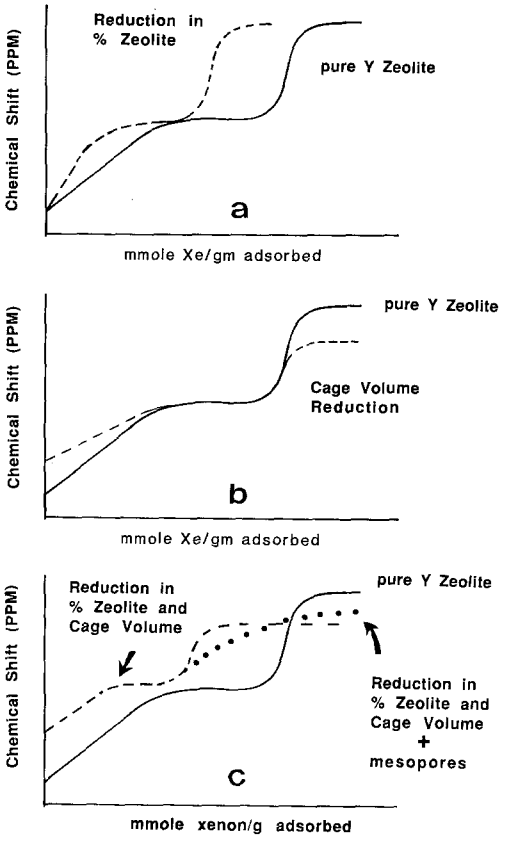

FIG. 5. (a) Solid line: σ curve of a Y zeolite with (+1) cation; dashed line: σ curve of a physical mixture of the zeolite with another material which does not absorb xenon. (b) Solid line: σ curve of the zeolite; dashed line: σ curve of the zeolite with smaller cage size but maintaining the same micropore capability. (c) Solid line: σ curve of the zeolite; dashed line: the combination of the dashed lines in a and b; dotted line: modification of the dashed line by the exchange of xenon between micropores and mesopores.

cage size (for instance by introducing foreign material into the supercages) while maintaining the same micropore capacity by increasing the numer of supercages per gram of sample (for instance by replacing the heavier cations in the sodalite cages with smaller (+1) cations). The chemical shift at the limit of zero xenon loading, σ_0, is larger than that of the original zeolite, while the chemical shift after the ^{129}Xe NMR endpoint, σ_e, is smaller. It has been shown that σ_0 is inversely proportional to the size of the supercage (*8, 11*) while σ_e is correlated to the free volume of the cage (*8*). The dashed line in Fig. 5c describes the combined effects of the above two situations and is a realistic representation of the steam-modified zeolite, where there are reductions in the cage size as well as the number of cages. If mesopores are present, xenon atoms will also adsorb into the mesopores at high xenon loadings. Then the σ curve is modified to the dotted line in the figure because the xenon density in the supercages increases slower with the xenon loading.

The evolution of the ^{129}Xe NMR spectra of the fresh catalysts with xenon loading is similar to those of Y zeolites with (+1) cations except that changes occur at lower loadings of xenon due to the dilution of the zeolite materials by the amorphous matrices. The σ curves may be divided into four

TABLE 1

Sample	σ_0 (ppm)	σ_e (ppm)	L_m (mmol Xe/gm)	L_e (mmol Xe/gm)
Fresh catalyst *A*	85	251	1.27	2.08
Equilibrium catalyst *A*	118	224	0.75	1.15
Fresh catalyst *B*	91	251	0.99	1.79
Equilibrium catalyst *B*	121	223	0.55	0.96
Fresh catalyst *C*	88	—	0.93	—
Equilibrium catalyst *C*	144	219	0.62	0.82

regions similar to that of the HY zeolite shown in Fig. 4. In region 1, at very low loadings of xenon, all three fresh catalysts show a single resonance. As the loading increases, multiple resonances are observed, leading to a large increase in the linewidth (only the chemical shift of the dominant resonance is shown in Figs. 1 to 4). In region 2, a further increase in xenon loading collapses the line back to a single resonance with much reduced width. The similarity of the spectra in region 1 and 2 between the fresh catalysts and Y zeolites confirms that xenon adsorbs first into the supercages.

On the other hand, only a single resonance is observed in the equilibrium catalysts in the same regions. This is similar to what we have observed in severely steam-dealuminated HY zeolites (*8*), indicating that hydrothermal conditions of catalytic cracking modify the zeolite content of the catalysts similarly. The plateau of the σ curve in region 2 in the equilibrium catalysts is highly compressed; its presence is sometimes difficult to resolve.

The chemical shift at the limit of zero xenon loading, σ_0, may be estimated by extrapolation of the initial two or three data points of the σ curve to zero loading. The results are given in Table 1. It should be emphasized that there are considerable uncertainties in these values due to low signal-to-noise ratios in the NMR spectra at the low-loading regime. Nevertheless, the values of σ_0 of the fresh catalysts are comparable to the value of 87 ppm observed in HY zeolite, and there are large increases in σ_0 of the equilibrium catalysts. Since σ_0 is inversely proportional to the average size of the supercage (*8, 11*) and increases with the broadening in the distribution of the cage size (*8*), our results suggest that there are reductions in the zeolite cage size in the equilibrium catalysts, probably due to occlusion by the reaction debris and by-products of the steam dealumination.

In region 3, the linewidth minimum can be clearly identified in all the catalysts (*12*). As in pure Y zeolites, it occurs just before the rapid increase in the xenon partial pressure in the xenon adsorption isotherm, and the chemical shift at the minimum is about 201 ppm. This suggests that up to this point, the ^{129}Xe NMR mainly reflects the properties of the zeolite cages and that the physical state of the adsorbed xenon at L_m in the catalysts is the same as it is in HY, NaY, and steamed-modified HY zeolites. However, the increase in the chemical shift at L_m is not as drastic as that in the Y zeolites. This is because after L_m, xenon begins to condense in the mesopores in addition to the supercages. Thus an increase in the xenon loading no longer leads to a commensurate

increase in the xenon density in the zeolite cages.

There are two groups of mesopores: those which are part of the zeolite particles and those in the amorphous matrices. We shall refer to them as the interior and exterior mesopores, respectively. Since the interior mesopores are close to the supercages, rapid exchange of xenon between the interior mesopores and the supercages can occur. The ^{129}Xe resonance at loadings greater than L_m in region 3 is the exchange average (*8*) of the signals from xenon atoms in supercages and those in the interior mesopores. On the other hand, xenon adsorbed in the exterior mesopores will produced separate signals.

In pure Y or steam-modified Y zeolites, solid xenon begins to form after the NMR end-point, L_e, in region 4 (that is, after the complete filling of the zeolite cages). In cracking catalysts, solid xenon will not form until all the exterior mesopores (which constitute a large fraction of the total pore volume) are filled, even though the filling of the supercages and interior mesopores has been completed. Therefore for the catalysts, the NMR end-point, L_e, of the xenon titration of the micropores may be more appropriately defined as the xenon loading at which the σ curve begins to level off to a constant value σ_e after region 3. The constancy of the chemical shift with increasing xenon loading after L_e implies that the xenon density in the micropores and interior mesopores no longer varies with loading as no additional xenon atoms can be accommodated.

The values of L_e and σ_e of the catalysts are summarized in Table 1 except for those of the fresh catalyst *C*. The fresh catalyst *C* is different from other catalysts in the way in which the zeolite cages are distributed through the supporting matrix. According to the catalyst manufacturers, both catalysts *A* and *B* are prepared by mixing Y zeolite (micron-sized particles) with an amorphous matrix. The exchange rate of xenon between zeolite particles and the pores of the matrix is slow and only xenon atoms adsorbed in the outer surface of the zeolite particles are involved. Therefore the resonance of the xenon atoms in the zeolite particles can be distinguished from that in the supporting matrix. This is shown in Fig. 6 for the equilibrium catalysts *A* and *B* at a xenon loading larger than L_e. The resonance of the xenon in the pores of the amorphous matrix (peak 2) is downfield from that in the zeolite particles (peak 1) and is at the location similar to that of xenon adsorbed in amorphous silica-alumina at high xenon loadings. (The *first* appearance of the resonance of the xenon in the support may be difficult to detect as it is masked by the signals from the xenon in the zeolite.) On the other hand, the zeolite in

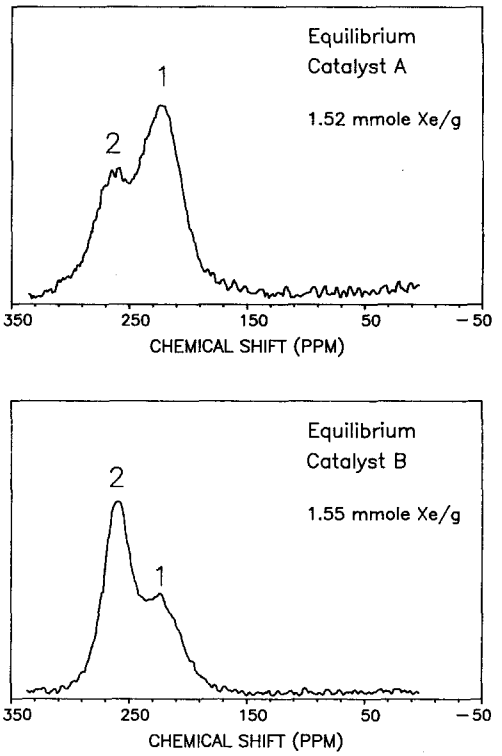

FIG. 6. ^{129}Xe NMR spectra of xenon adsorbed in equilibrium catalysts *A* and *B* at 144 K at a xenon loading larger than L_e. Peaks 1 and 2 correspond, respectively, to xenon in the zeolite particles and in the pores of the amorphous support.

catalyst *C* is grown *in situ* from the matrix itself. Each individual zeolite "particle" contains few supercages. Exchange of xenon atoms between the zeolite cages and the matrix is rapid at high xenon loadings, where the heat of adsorption of xenon per xenon atom in the cages is greatly reduced. The ^{129}Xe resonance at high xenon loadings is the average of that in the zeolite cages and in the pores of the support. The second resonance similar to those in Fig. 6 is not observed. The xenon chemical shift will continue to increase (shifting downfield) with increasing loading until most of the mesopores of the support are filled. Since the pores of the support contribute to a large fraction of the total pore volume of the catalyst, at the complete filling of the pores of the support, the NMR signals from the xenon in the zeolite make only insignificant contributions to the total signal.

The difference between the fresh and equilibrium catalyst *C* may be due to the smaller zeolite cage size in the latter. Smaller cage size leads to larger heat of adsorption (*13, 14*) of xenon and reduces the exchange of xenon between the zeolite and matrix.

Zeolite Content in Cracking Catalysts

The zeolite content of a cracking catalyst can be characterized by two parameters: (1) the number of supercages; (2) the average size of the cages. The total micropore capacity, L_{mi}, of a catalyst, which is primarily due to the supercages, can be determined directly from the xenon loading at the linewidth minimum, L_m. We have shown (*8*) that at L_m, xenon density in the supercages is a constant since the adsorbed xenon is in the same physical state as reflected by the similar chemical shifts at the linewidth minimum for pure Y and steam-modified Y zeolites. Then using the xenon density in HY zeolite (at the L_m of HY zeolite), we find that

$$L_{mi} = \xi L_m, \quad (1)$$

where the constant ξ equals to L_e(HY)/L_m(HY) = 10/8.25. The origin of ξ is discussed in detail in Ref. (*8*). It is due to the fact that complete filling of the supercages by xenon does not occur until the xenon loading is equal to or larger than L_e. Additional xenon atoms are adsorbed into the supercages at xenon loadings between L_m and L_e. ξ is a correction factor to account for this additional adsorption and is the same whether the Y zeolite is in a physical mixture with a supporting matrix or in the pure form. Values of L_{mi} for the catalysts are given in Table 2. It is clear that the zeolite supercage capacities are substantially smaller in the equilibrium catalysts. The reduction is due to two factors: (1) decrease in the number of supercages; (2) decrease in the free volume of the supercages. The decrease in the number of supercages is caused by the destruction of the zeolite by severe steaming conditions and vanadium in the feedstocks. The decrease in the free volume is mainly due to debris in the cages resulting from steam-dealumination and coke formation. The average cage size, V_e, given in terms of number of xenon atoms per cage, can be estimated (*8*) by first determining the chemical shift of xenon in completely filled supercages in the catalyst, σ_{mi}, and then reading off the cage size corresponding to the σ_{mi} from the xenon titration curve of the HY zeolite. σ_{mi} is calculated from σ_e and L_m using the equation

$$\sigma_e = (L_{mi}/L_e)\sigma_{mi} + (1 - L_{mi}/L_e)\sigma_{me}, \quad (2)$$

where σ_{me} is the chemical shift of xenon in completely filled interior mesopores and is estimated to be about 263 ppm from amorphous silica-alumina. Equation (2) indicates that the observed σ_e at the NMR end-point is the exchange average of the chemical shifts from the completely filled supercages and interior mesopores. The values of V_e in Table 2 show that the average cage size is indeed smaller in the equilibrium catalysts than in the fresh catalysts, and the reduction is about the same for catalysts *A* and *B*. The numbers of supercages, *n*, in the catalysts

TABLE 2

Sample	Micropore capability L_{mi}	Micropore size V_e	Number micropores n	% zeolite
Fresh catalyst *A*	1.54[a](41.4 × 10^{-3})[b]	9.1[c](406)[d]	169[e]	26
Equilibrium catalyst *A*	0.91(24.5 × 10^{-3})	8.4(375)	108	16
Fresh catalyst *B*	1.20(32.2 × 10^{-3})	9.1 (406)	133	20
Equilibrium catalyst *B*	0.67(18.0 × 10^{-3})	8.2(366)	81	12
Fresh catalyst *C*	1.13(30.4 × 10^{-3})	—	125[f]	19[f]
Equilibrium catalyst *C*	0.75(20.2 × 10^{-3})	8.4(375)	89	14

[a] In units of mmol Xe/g.
[b] In units of cm^3/g (assuming a volume of 44.6 $Å^3$ for a xenon atom).
[c] In units of xenon atoms per micropore.
[d] In units of $Å^3$ per micropore (assuming a volume of 44.6 $Å^3$ for a xenon atom).
[e] In units of μmol micropores/g.
[f] Assuming V_e = 9 xenon atoms/micropore.

are also shown in Table 2. They are calculated from the relation

$$L_{mi} = n \times V_e. \quad (3)$$

Clearly, the loss of the micropore capacity, and thus of the zeolite content, in the equilibrium catalysts is largely due to the destruction of the supercages; the role of the decrease in the cage size is only secondary. As mentioned above, we are unable to determine L_e and σ_e for the fresh catalyst *C*. However, from the results of fresh catalysts *A* and *B*, we may estimate V_e to be roughly nine xenon atoms/cage for the fresh catalyst *C*. With this approximation, the number of cages in the catalyst can be calculated from Eq. (3) and is included in Table 2. One sees that the percentage of the reduction in the number of zeolite cages between the fresh and equilibrium catalysts is about the same among the three cracking catalysts.

It is convenient to express the zeolite content in the catalysts in terms of percentage of zeolite, which is defined as 100% × (the ratio of the number of supercages in the catalyst to that if the catalyst were 100% HY zeolite). The results are shown in the last column in Table 2, where we have used the fact that there are 0.65 mmol of supercages per gram of HY zeolite. There are other methods to determine the percentage of zeolite in a cracking catalyst, such as nitrogen adsorption isotherm measurements. However, most of these methods are based on the *amount* of adsorbate, which depends on the number of the zeolite cages as well as the average size of the cages. The percentage of zeolite given here depends only on the *number* of zeolite supercages.

IV. CONCLUSION

We have shown that considerable information about the supercages (or micropores) of the zeolite in cracking catalysts can be extracted from low-temperature ^{129}Xe NMR. The results on the total micropore capability, L_m, the percentage zeolite, the number of supercages, n, and finally the supercage size, V_e, all provide different levels of characterization of a catalyst. By com-

paring the ^{129}Xe NMR data between a fresh and an equilibrium catalysts, changes in the zeolite content can be monitored.

REFERENCES

1. Ito, T., and Fraissard, J. P., *in* "Proceedings of the Fifth International Conference of Zeolites, Naples," pp. 510–515. Heyden, London, 1980.
2. Ito, T., and Fraissard, J. P., *J. Chem. Phys.* **76,** 5225 (1982) *J. Chem. Soc. Faraday Trans. 1* **83,** 451 (1987).
3. de Menorval, L. C., Fraissard, J. P., and Ito, T., *J. Chem. Soc. Faraday Trans. 1* **78,** 403 (1982).
4. Ito, T., de Menorval, L. C., Guerrier, E., and Fraissard, J. P., *Chem. Phys. Lett.* **111,** 271 (1984).
5. Springuel-Huet, M. A., Ito, T., and Fraissard, J. P., *in* "Proceedings, Congr. Structure and Reactivity of Modified Zeolites, Prague." Elsevier, Amsterdam, 1984.
6. Scharpf, E. W., Crecely, R. W., Gates, B. C., and Dybowski, C. R., *J. Phys. Chem.* **90,** 9 (1986).
7. Cheung, T. T. P., Fu, C. M., and Wharry, S., *J. Phys. Chem.* **92,** 5170 (1988).
8. Cheung, T. T. P., Fu, C. M., *J. Phys. Chem.* **93,** 3740 (1989).
9. Cheung, T. T. P., *J. Phys. Chem.* **94,** 376 (1990).
10. Jameson, C. J., Jameson, A. K., and Cohen, S. M., *J. Chem. Phys.* **59,** 4540 (1973).
11. Demarquay, J., and Fraissard, J., *Chem. Phys. Lett.* **136,** 314 (1987); Fraissard, J., Ito, T., Springuel-Huet, M., and Demarquay, J., *in* "Proceedings of the Seventh International Zeolite Conference, Tokyo," pp. 393–400. Elsevier, Amsterdam, 1986.
12. There is a second minimum in the linewidth in the equilibrium catalyst *B* at a higher xenon loading. It occurs just before the adsorption of xenon in the exterior mesopores of the support matrix. The broadening after the minimum is due to the presence of multiple resonances from xenon adsorbed in the zeolite particles and in the amorphous support.
13. See for instance, "Adsorption, Surface Area and Porosity" (S. J. Gregg and K. S. W. Sing). Academic Press, London, 1982.
14. Derouane, E. G., Andre, J-M. and Lucas, A. A., *Chem. Phys. Lett.* **137,** 336 (1987).